ISSN 1807-1929
Revista Brasileira de Engenharia Agrícola e Ambiental
Brazilian Journal of Agricultural and Environmental Engineering
v.26, n.8, p.564-570, 2022
Campina Grande, PB – http://www.agriambi.com.br – http://www.scielo.br/rbeaa

DOI: http://dx.doi.org/10.1590/1807-1929/agriambi.v26n8p564-570

Calibration of simulation parameters for wind erosion gas-solid two-phase flow in arid and semiarid soils[1]

Calibração de parâmetros de simulação para a erosão eólica fluxo de gás sólido em duas fases em solos áridos e semiáridos

Baoer Hao[2], Xin Tong[2], Zhi Chen[2*] & Haiyang Liu[2]

[1] Research developed at Inner Mongolia Agricultural University, Hohhot, Inner Mongolia Autonomous Region, PR China
[2] Inner Mongolia Agricultural University, Hohhot, Inner Mongolia Autonomous Region, PR China

HIGHLIGHTS:

Providing accurate soil physical parameters is essential in the coupled simulation of wind and sand two-phase flow.
The Hertz-Mindlin and JKR contact models in EDEM could be used to accurately calibrate soils in arid and semiarid regions.
The threshold wind velocity could accurately reflect the error between the actual measurement and simulation.

ABSTRACT: To construct a coupled simulation model of soil wind erosion and two-phase flow in arid and semiarid regions, the proper contact parameters of the soil discrete element simulation model are obtained based on the angle of repose (AoR) calibration test. The coupled simulation model is established by combining computational fluid dynamics. The response value of the wind speed of sand initiation is used to verify the model's accuracy. Due to the characteristics of arid and semiarid soils, this paper uses the Hertz-Mindlin with JKR contact model in EDEM software to calibrate the soil parameters based on soil physical tests and designs the Plackett-Burman, steepest climb, and Box-Behnken tests according to Design-Expert software to obtain the soil AoR second-order regression. With the AoR of 33.52° as the target, the best combination of parameters is obtained: soil-soil collision recovery of 0.64, soil-steel static friction coefficient of 0.31, JKR surface energy of 3.302 J m^{-2}. Finally, by using calibrated parameters and the threshold wind velocity as the response value, the wind-sand air-solid two-phase flow test is conducted in ANSYS Fluent and EDEM, with the relative error between the starting wind speed recorded by the high-speed camera in the wind tunnel test and the threshold wind velocity shown in the simulation model calculated to be 8.7%, and the calibrated soil parameters met the requirements of the coupled simulation.

Key words: discrete element, two-phase flow, angle of repose, soil

RESUMO: Para construir um modelo de simulação acoplada da erosão eólica do solo e fluxo bifásico em regiões áridas e semi-áridas, os parâmetros de contato apropriados do modelo de simulação de elementos discretos do solo são obtidos com base no teste de calibração do ângulo de repouso (AoR). O modelo de simulação acoplado foi estabelecido através da combinação da dinâmica computacional dos fluidos. O valor de resposta da velocidade do vento de iniciação da areia foi usado para verificar a precisão do modelo. Devido às características dos solos áridos e semi-áridos, este trabalho usa o modelo de contato Hertz-Mindlin com JKR no software EDEM para calibrar os parâmetros do solo com base nos testes físicos do solo, e projeta o Plackett-Burman, a subida mais íngreme, e os testes Box-Behnken de acordo com o software Design-Expert para obter a regressão de segunda ordem do AoR do solo. Com o AoR 33,52° como alvo, obtém-se a melhor combinação de parâmetros: recuperação de colisão solo-solo 0,64, coeficiente de atrito estático solo-aço 0,31, energia de superfície JKR 3,302 J m^{-2}. Finalmente, usando parâmetros calibrados e a velocidade do vento inicial como valor de resposta, o teste de fluxo de ar e vento sólido de duas fases foi conduzido em ANSYS Fluent e EDEM, com o erro relativo entre a velocidade do vento inicial registrada pela câmera de alta velocidade no teste de túnel de vento e a velocidade do vento inicial mostrada no modelo de simulação calculada em 8,7%, e os parâmetros calibrados do solo atenderam aos requisitos da simulação acoplada. Os resultados da simulação indicam que os parâmetros de calibração do solo podem ser utilizados para modelar a erosão do vento em duas fases do solo em ambientes semi-áridos.

Palavras-chave: elemento discreto, fluxo em duas fases, ângulo de repouso, solo

• Ref. 258129 – Received 10 Nov, 2021
* Corresponding author - E-mail: sgchenzhi@imau.edu.cn
• Accepted 15 Mar, 2022 • Published 04 Apr, 2022
Editors: Geovani Soares de Lima & Hans Raj Gheyi

Introduction

Soil wind erosion is an erosion process in which wind-dominated external camp forces act on the ground and cause the flying, jumping, and rolling of dust and sand, leading to soil loss in arid and semiarid regions (Kamali et al., 2020). Using the discrete element method, which can reflect the interaction between fundamental particles, including bonding, separation, slipping, and rolling between particle units, provides a new idea to study the complex dynamic behavior of soil. (Li, 2015).

Soils have more complex particle properties than other materials, and their properties are affected by changes in moisture, organic matter, and microorganisms. Therefore, even the model and parameters of soil particles with the same properties still need to be modeled and calibrated separately according to the actual conditions to ensure the accuracy of subsequent simulation studies (Zeng et al., 2021). Internal friction and cohesion between soils are critical soil parameters that affect wind erosion (Dai et al., 2020). Xiang et al. (2019) constructed a soil discrete element simulation model using the JKR model to obtain accurate contact parameters for the discrete element simulation model of a southern China clay loam soil. Ucgul et al. (2015) used the discrete element method to propose the hysteretic spring contact model to solve the soil force-plastic deformation problem.

The DEM-CFD coupled simulation method is used to study the kinetic characteristics of the soil in the wind action and the mechanical properties between soil particles. The Hertz-Mindlin with JKR model is chosen, and the required parameters are accurately calibrated. This research provides a reference basis for studying the discrete element simulation parameters of soil wind erosion in arid and semiarid areas.

Materials and Methods

The primary sampling site for this study is located in Siziwang, which is part of Ulanqab City in the central Inner Mongolia Autonomous Region of China, with a geographical location between 41°10' to 43°22' N latitude and 110°20' to 113° E longitude, 1000~1200 m above sea level. Kastanozem has a humus layer 15~40 cm thick and organic matter content of less than 1%. The topography includes dunes, basins, and desert grasslands, with relatively flat terrain, which is typical for an arid and semiarid region, as shown in Figure 1.

The soil samples were sampled at the test site using the cutting ring method of five-point sampling, the moisture content was determined to be 1.65% using the drying experiment, and the soil density was measured as 2.130 kg dm^{-3} using the pycnometer test method (Viana et al., 2020). As shown in Figure 2, the soil was sieved, and the percentage of soil particle size distribution was determined (Table 1) according to the soil classification criteria (Wu, 2016). According to the soil mechanical composition classification criteria, it was concluded that the particles larger than 0.075 mm accounted for 86% of the total mass, and the test soil samples were classified as fine sand.

Due to the large variability of physical soil parameters caused by different soil types, accurate calibration and optimization were required by using both the soil sample intrinsic and simulation parameter calibration methods.

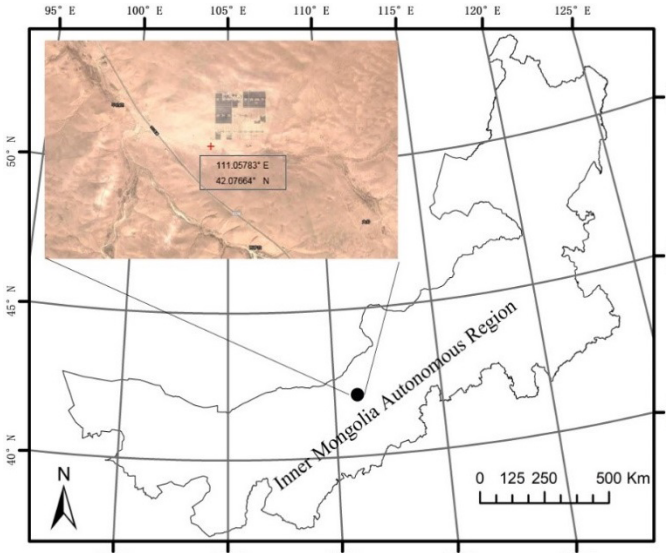

Figure 1. The geographical location of the study area

Figure 2. Soil screening

Table 1. Percentage of soil particle size distribution

Soil particle size (mm)	Soil percentage (%)
< 0.25	52.96
0.25~0.5	18.56
0.5~1	8.53
1~2	2.83
> 2	16.93

A ZJ-type strain-controlled straight shear instrument was used to measure mechanical parameters such as the angle of internal friction and cohesion of the test soil and further analyze the lateral pressure coefficient and Poisson's ratio of the test soil (Chen, 2014). Cohesion 2.03 and angle of internal friction 36.13° were obtained from the relationship between the soil shear strength and vertical pressure (Sun, 2010).

The soil lateral pressure coefficient for the internal friction angle of the soil was approximated using Eq. 1 (Cheng et al., 2003).

$$k_0 = 1 + \sin\varphi \quad (1)$$

where:

k_0 - soil lateral pressure coefficient.

φ - angle of repose, °.

The value of Poisson's ratio was then estimated according to Eq. 2 (Xu et al., 2017), the soil shear modulus was then obtained. The shear modulus of the test soil was obtained as 2×10^{10} kPa.

$$\mu = \frac{k_0}{1 + k_0} \quad (2)$$

$$G = \frac{E}{2(1+\mu)} \quad (3)$$

where:

G - shear modulus, t m^{-2};

E - modulus of elasticity, MPa;

μ - Poisson's ratio.

As shown in Figure 3, the test uses the CNY-1 inclinometer to measure the friction coefficient between soil-steel and soil-soil, to record the inclination angle, and uses the angle to calculate the friction coefficient. Each group of experiments was repeated 20 times, and the static friction coefficient was determined to be 0.61 ± 0.25 for soil-soil and 0.34 ± 0.26 for soil-steel. The rolling friction coefficient was determined to be 0.69 ± 0.43 for soil-soil and 0.41 ± 0.20 for soil-steel.

The test was performed by an FT-104B repose angle measuring instrument, and the test setup is shown in Figure 4. The stacking test was repeated ten times, and the average value was recorded as the AoR in the physical soil test, which was 33.52° with a standard deviation of 0.68°.

The soil AoR simulation test is shown in Figure 5. A virtual plane was generated at the top of the funnel to generate soil particles. The soil particles were dropped at a rate of 2 m s^{-1}, and the test was completed until all soil stopped moving to the base plate. The binarization, boundary extraction and edge fitting of the single-sided image with superimposed angles were performed using MATLAB to finally obtain the AoR; the values of the simulation parameters are shown in Table 2.

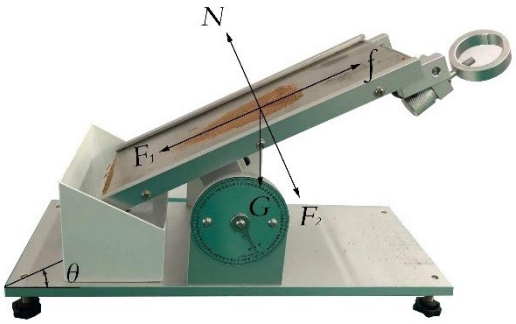

F_1 - The tensile force, [N]; F_2 - The pressure, [N]; G - The gravity, [N]; f - The friction, [N]; θ - The inclination angle of the inclinometer, (°)

Figure 3. CNY-1 incline instrument soil rolling friction test

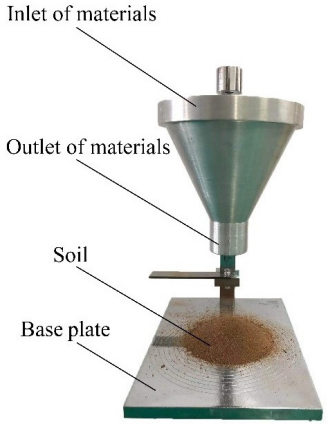

Figure 4. The angle of repose test

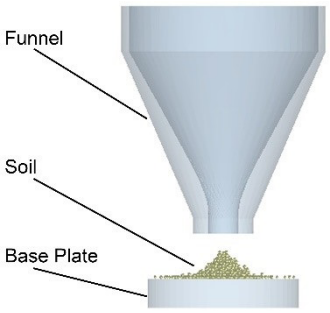

Figure 5. Angle of repose simulation test

Table 2. Simulation test parameters

Simulation test parameters	Value
Shear modulus of soil	2.05 × 10^{10} kPa
Density of soil	2.130 kg dm^{-3}
Poisson's ratio of soil	0.29
Shear modulus of steel	7 × 10^{7} kPa
Density of steel	7850 kg m^{-3}
Poisson's ratio of steel	0.30
Soil-soil restitution coefficient	0.60
Soil-soil static friction coefficient	0.61
Soil-soil rolling friction coefficient	0.69
Soil-steel restitution coefficient	0.25
Soil-steel static friction coefficient	0.34
Soil-steel rolling friction coefficient	0.41
Surface energy of soil for JKR model	3 J m^{-2}

The experimental design was carried out in Design-Expert. Based on the Plackett-Burman test, the steepest climbing test was conducted for the three significant parameters screened. The results of the steepest climbing test: tests 1, 2 and 3 were coded as high (+1), medium (0), and low (-1) levels. Finally, the results of the Box-Behnken test were subjected to multiple regression analysis to obtain the second-order regression equation for the AoR of the soil simulation test.

Physical tests of the threshold wind velocity were performed in a wind tunnel. As shown in Figure 6, the wind tunnel is an OFDY-1.2 type movable wind erosion wind tunnel, with a total length of 11.8 m, a test section length of 7.2 m, a shrinkage rate of 1.7, a wind tunnel working section of 1.2 × 1.0 m, and a boundary layer thickness of 1.5 m; the wind speed was adjustable in the range of 0~18 m s^{-1}, which can simulate the natural wind speed. Lighting with a high-brightness LED light source was installed on the wind tunnel wall; a resolution is 2016 × 2016, frame rate black and white was 1279 and the number of pictures is 6307 German PCO DimaxS high-speed camera was placed outside the test section to record the movement of sand grains. First, the test soil was spread thinly in the wind tunnel test section, and then the wind tunnel was adjusted to six different wind speeds of 5, 5.5, 6, 6.5, 7 and 7.5 m s^{-1}. During the 5 s of blowing, the photos of the soil samples being blown were recorded separately. The pictures of the soil samples being eroded were recorded, and the different wind speed erosion tests were repeated three times to take the average wind speed of the sand.

Results and Discussion

The Plackett-Burman parameters are selected in the range shown in Table 3, and the test protocols and results are shown

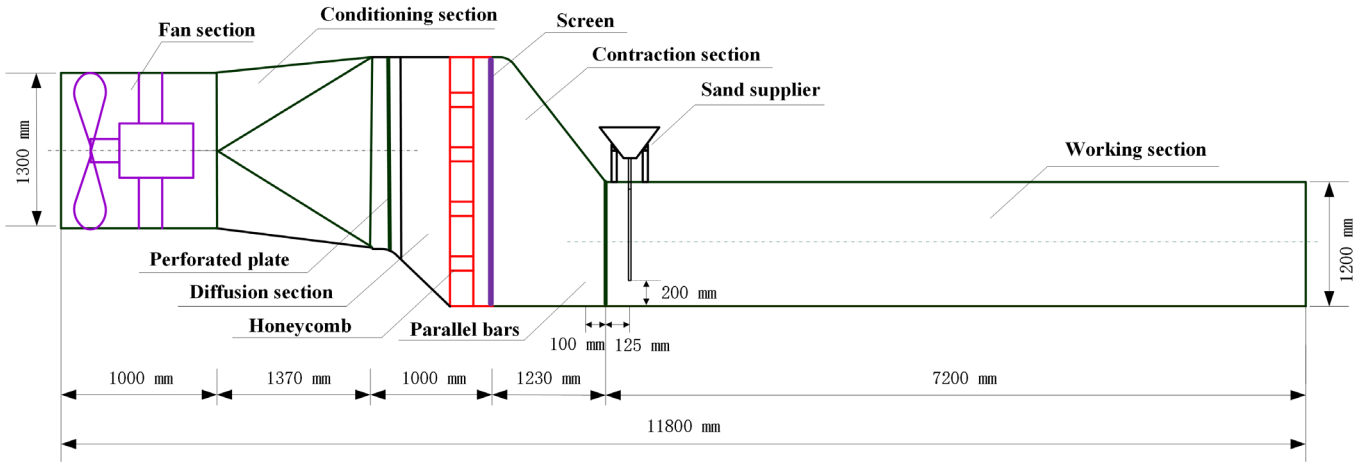

Figure 6. Diagram of the OFDY-1.2-type wind tunnel

Table 3. Simulation test parameters

Symbol	Simulation test parameters	Low level (-1)	High level (+1)
At	Shear modulus of soil	1.00	3.00
Bt	Poisson's ratio of soil	0.10	0.50
Ct	Soil-soil restitution coefficient	0.40	0.80
Dt	Soil-soil static friction coefficient	0.40	0.80
Et	Soil-soil rolling friction coefficient	0.50	0.90
Ft	Soil-steel restitution coefficient	0.05	0.45
Gt	Soil-steel static friction coefficient	0.15	0.55
Ht	Soil-steel rolling friction coefficient	0.20	0.60
It	Surface energy of soil for JKR model/(J m^{-2})	2.50	3.50

in Table 4. The ANOVA results and the significant effects of the simulation parameters are shown in Table 5. The significance of the static friction coefficient between the soil and steel is less than 0.01, which has a substantial effect on the simulation AoR; the relevance of the soil-soil collision recovery coefficient and JKR surface energy is less than 0.05, which has a significant impact on the simulation AoR; and the other parameters have minimal effects on the test.

The steepest climbing test protocol and results are shown in Table 6. The relative error of soil AoR tends to decrease from high values and then increase. The relative error of AoR reaches the minimum value at the level of test Nº 2, and the optimal interval of the test can be determined to be near test Nº 2. The Box-Behnken test is conducted with test Nº 2 as an intermediate level, test Nº 1 as a high level, and test Nº 3 as a low level.

Table 5. Results of variance analysis of the Plackett-Burman test

Parameters	Degree of freedom	Sum of squares	F value	P value
At	1	81.64	3.18	0.1727
Bt	1	5.91	0.2299	0.6644
Ct	1	851.43	33.13	0.0104*
Dt	1	10.08	0.3923	0.5755
Et	1	197.64	7.69	0.0694
Ft	1	129.89	5.05	0.1101
Gt	1	1937.51	75.39	0.0032**
Ht	1	19.56	0.7610	0.4472
It	1	335.60	13.06	0.0364*

Note: ** - shows that the impact is highly significant ($p < 0.01$), and * - shows that the impact is significant ($p < 0.05$). For details of parameters see Table 3

Table 6. Result of steepest climbing test design scheme

Nº	Soil–soil restitution coefficient	Soil-steel static friction coefficient	Surface energy of soil for JKR model	Repose angleθ/(°)	Relative error/%
1	0.80	0.15	3.5	31.51	6.00
2	0.72	0.23	3.3	32.21	3.90
3	0.64	0.31	3.1	29.68	11.40
4	0.56	0.39	2.9	43.83	30.75
5	0.48	0.47	2.7	45.84	36.75
6	0.40	0.55	2.5	51.56	53.81

The Box-Behnken test was performed based on the results of the steepest climb test (Table 7), and the experimental design is shown in Table 8. The results show that Ct, It and

Table 4. Plackett-Burman test scheme and results

Nº.	Parameters									Repose angle θ/(°)
	At	Bt	Ct	Dt	Et	Ft	Gt	Ht	It	
1	1	1	-1	1	1	1	-1	-1	-1	32.03
2	-1	1	1	-1	1	1	1	-1	-1	47.98
3	1	-1	1	1	-1	1	1	1	-1	32.21
4	-1	1	-1	1	1	-1	1	1	1	43.83
5	-1	-1	1	-1	1	1	-1	1	1	6.84
6	-1	-1	-1	1	-1	1	1	-1	1	48.49
7	1	-1	-1	-1	1	-1	1	1	-1	51.00
8	1	1	-1	-1	-1	1	-1	1	1	12.95
9	1	1	1	-1	-1	-1	1	-1	1	13.49
10	-1	1	1	1	-1	-1	-1	1	-1	6.27
11	1	-1	1	1	1	-1	-1	-1	1	3.43
12	-1	-1	-1	-1	-1	-1	-1	-1	-1	23.00
13	0	0	0	0	0	0	0	0	0	33.82

For details of parameters see Table 3

Table 7. Levels coding table of the parameter

Levels	Soil-soil restitution coefficient	Soil-steel static friction coefficient	Surface energy of soil for JKR model
-1	0.80	0.15	3.5
0	0.72	0.23	3.3
+1	0.64	0.31	3.1

Table 8. Results of the Box-Behnken test scheme

Nº	Soil-soil restitution coefficient	Soil-steel static friction coefficient	Surface energy of soil for JKR model	Repose angle θ/(°)
1	-1	-1	0	20.75
2	1	-1	0	20.12
3	-1	1	0	33.62
4	1	1	0	31.12
5	-1	0	-1	20.27
6	1	0	-1	19.79
7	-1	0	1	23.75
8	1	0	1	20.81
9	0	-1	-1	12.95
10	0	1	-1	26.10
11	0	-1	1	16.17
12	0	1	1	24.23
13	0	0	0	26.80
14	0	0	0	26.11
15	0	0	0	24.95
16	0	0	0	26.51
17	0	0	0	25.12

GtIt are significant, as shown in Table 9, and the effect of Gt and It^2 on the AoR is highly significant; the equation model is highly significant ($p < 0.0001$), and the misfit term P = 0.4654 is insignificant, indicating that the regression fitting model is accurate. The coefficient of determination of the regression equation $R^2 = 0.9883$ and the corrected coefficient of determination of $R^2adj = 0.9731$, both of which are approximately equal to 1, indicate that the fitted equation is credible, and the coefficient of variation of CV% = 3.55 and the accuracy reach 32.9751, suggesting that the model has good accuracy.

The second-order regression equation for the AoR of the soil simulation test is as follows:

$$\theta = 25.90 - 0.8187Ct + 5.64Gt + 0.7313It + 0.4675CtGt - 0.615CtIt - 1.27GtIt + 0.8985Ct^2 - 0.3940Gt^2 - 5.64It^2$$

$$R^2 = 0.9883$$

Table 9. Variation analysis of the Box-Behnken test quadratic model

Source	Mean square	Degree of freedom	Sum of square	P value
Model	409.90	9	45.54	< 0.0001**
Ct	5.36	1	5.36	0.0275*
Gt	254.03	1	254.03	< 0.0001**
It	4.28	1	4.28	0.0423*
CtGt	0.8742	1	0.8742	0.2994
CtIt	1.51	1	1.51	0.1839
GtIt	6.48	1	6.48	0.0186*
Ct^2	3.40	1	3.40	0.0628
Gt^2	0.6536	1	0.6536	0.3648
It^2	134.01	1	134.01	< 0.0001**
Residual	4.87	7	0.6961	
Lack of fit	2.41	3	0.7118	0.4654
Pure error	2.74	4	0.6843	
Sum	414.77	16		

In this experiment, the soil AoR was used as the evaluation index for the calibration of the soil simulation model parameters, and the model data were fitted by quadratic multiple regression using Design-Expert software. The response surface and contour distribution of the interactions between the parameters affecting the AoR and the objective function were obtained, as shown in Figure 7. The slope of the response surface in Figure 7 was relatively large, meaning that the change in CtGt, CtIt, and GtIt has a more significant impact on the AoR; at the same time, as shown in Figures 7B and C, the CtIt and GtIt contour lines present a larger curvature ellipse, indicating that the interaction influence was substantial. As shown in Figure 7A, the curvature of the contour is gentle, indicating that the CtGt interaction was not significant.

The simulation regression model was optimized based on the optimization module in Design-Expert software and using the measured AoR 33.52° from the physical tests as the target parameter. Among the 100 sets of solutions derived from the software, the parameters that are similar to the physical test results are selected: soil-soil collision recovery 0.64, soil-steel static friction coefficient 0.31, JKR surface energy 3.302 J m^{-2}, and the rest of the parameters were simulated using Box-Behnken test parameters as the standard. The soil AoR was obtained by repeating three times: 33.02°, 32.52°, 33.18°, with an average value of 32.91°, and the relative error between the AoR and the actual 33.52° measured AoR is 1.82%. A two-

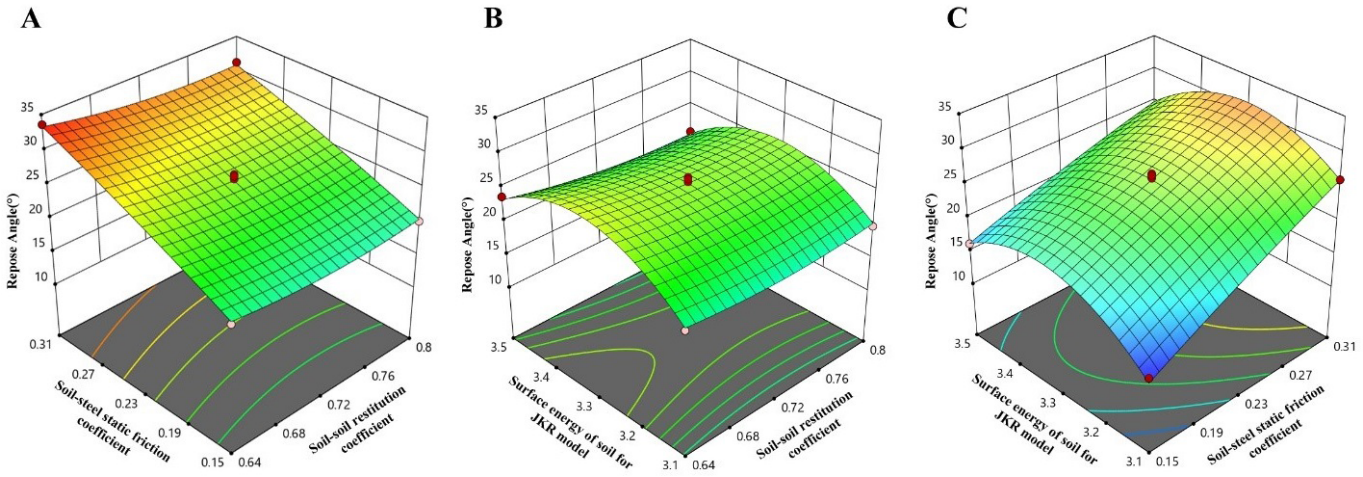

Figure 7. Interaction between the parameters affecting repose angle

sample T test of the sample and the physical test AoR yielded a p = 0.10497, which shows no significant difference between the two samples at 0.05 probability level. The results are shown in Figures 8A and B.

Experiments were conducted in the wind tunnel and DEM-CFD to verify the accuracy of the soil discrete element calibration parameters in CFD coupled wind-sand two-phase flow simulation tests. The threshold wind velocity was used as the response value to compare and analyze the wind tunnel wind velocity with the simulated wind velocity, and the model's accuracy was determined by the relative inaccuracy of the two test results.

The threshold wind velocity was found to be between 6~7 m s^{-1} through the high-speed camera in the wind tunnel test, and the actual threshold wind speed was calculated to be 6.9 m s^{-1} based on the number of frames per second taken by the high-speed camera, as shown in Figure 9.

Simulation tests were performed by coupling the DEM-CFD method. ANSYS SCDM software was used to build the wind tunnel model according to the scale 2:1 and draw the mesh. The MESH file was imported into EDEM software (Zhou et al., 2017; Ding et al., 2019), the wind tunnel material was steel, and the intrinsic parameters are Poisson's ratio 0.3, density 7850 kg m^{-3}, and shear modulus 7.0 × 10^7 kPa. Then, according to the above soil calibration results, the soil particle model was built, and the EDEM time step was set to 4e × 10^{-7} s. The parameter settings were saved, and the coupling interface was opened. Import the API coupling interface in ANSYS FLUENT; at this time, the data interface between the two software programs was opened, and data exchange coupling could be carried out; adopting the Eulerian model, the wind tunnel inlet velocity of 6~7 m s^{-1} was set to ten groups of simulations with 0.1 m s^{-1} as the wind speed interval for the test, set the outlet as the pressure outlet, the FLUENT time step size is assigned to 4e × 10^{-5} s, and the number of time steps is set to 100000 degrees, i.e., the simulation time was 4 s. To obtain accurate information on soil particle movement, each time step was assigned to a maximum of 30 iterations, and the data were saved every 0.05 s in EDEM and FLUENT. The results show that the coupled simulation results are in basic agreement with the physical test, and the sand starts to move when the wind speed is 6.3 m s^{-1}.

Figure 8. AoR comparison chart (A: AoR of the simulation test, B: AoR of the physical test.)

Figure 9. High-speed camera shooting process

The wind speed of sand initiation is limited by various conditions, such as soil particle size and moisture. Studies on the observation method of threshold wind velocity and its influencing factors showed that the range of threshold wind velocity is 5.5~12 m s^{-1} (Wang et al., 2007). The study of the application of high-speed photography in the measurement of wind and sand particle velocity using the high-speed camera, multiframe image matching method, and a wind speed of 6.9 m s^{-1} is observed for threshold wind velocity (Jiang et al., 2017). The relative error is 8.7% compared to the threshold wind velocity of 6.3 m s^{-1} in the coupled DEM-CFD blowing experiment. Soil calibration parameters reflect the physical properties of the soil and meet the requirements of coupled simulation.

Since the physical calibration process of the soil contains several parameters, each of them has its own error value, and these errors accumulate in the final test, which is one of the reasons for the difference between the wind tunnel test and the simulation test. In addition, because the soil model in the simulation process is a single sphere and most of the soil particles are irregular in shape, this is also the reason for the error between the physical experiment and the simulation experiment. However, this difference is relatively small and does not affect the application of this calibration scheme in soil wind erosion research. The soil calibration parameters derived in this study can be used to simulate two-phase flow simulations of wind erosion, water erosion, etc., in soils with similar textures over a large range.

Conclusions

1. The optimal combination of simulation parameters is used to repeat the validation test, and the relative error between the simulated AoR and the measured AoR is 1.82%.

2. With the threshold wind speed as the response value, the measured wind velocity is compared with the coupled CFD-DEM simulation wind velocity, and the relative error between them is 8.7%.

3. More importantly, the method presented in the article can be used for soil calibration in other wind and water erosion areas to enable the simulation of events.

Literature Cited

Chen, Z. Research on the basic theory of unsaturated soil and special soil mechanics. Chinese Journal of Geotechnical Engineering, v.36, p.201-272, 2014.

Cheng, Y. P.; Nakata, Y.; Bolton, M. D. Discrete element simulation of crushable soil. GéoTechnique, v.53, p.633-641, 2003.

Dai, J.; Lu, G.; Du, X. Soil anti-erodibility and its relationship with mechanical properties in aeolian sandy land in northwestern Liaoning. Journal of Hulunbeier University, v.28, p.65-72, 2020.

Ding, H.; Shi, J.; Ma, X. Simulation experiment of grain vertical airflow winnowing based on DEM-CFD coupling. Journal of Gansu Agricultural University, v.54, p.190-197, 2019. https://doi.org/10.13432/j.cnki.jgsau.2019.06.026

Jiang, C.; Wang, X.; Dong, Z. Research on application of high-speed photography technology in velocity measurement of sand particles. Arid Land Geography, v.40, p.746-753, 2017. https://doi.org/10.13826/j.cnki.cn65-1103/x.2017.04.005

Kamali. N.; Siroosi, H.; Sadeghipour, A. Impacts of wind erosion and seasonal changes on soil carbon dioxide emission in southwestern Iran. Journal of Arid Land, v.12, p.690-700, 2020. https://doi.org/10.1007/s40333-020-0018-5

Li, L. Research status and the prospect of discrete element method in agricultural engineering. Chinese Journal of Agricultural Mechanization Chemistry, v.36, p.345-348, 2015. https://doi.org/10.13733/j.jcam.issn.2095-5553.2015.05.084

Sun, H.Y. Guidance of soil mechanics experiments. Beijing: China Water Power Press, 2010. Cap.10, p.76-92.

Ucgul, M.; Fielke, J. M.; Saunders, C. Three-dimensional discrete element modeling (DEM) of tillage: accounting for soil cohesion and adhesion. Biosystems Engineering, v.129, p.298-306, 2015. https://doi.org/10.1016/j.biosystemseng.2014.11.006

Viana, J. R.; Macêdo, AAM.; Santos, A.; Façanha Filho, P. de F.; Silva, C. Análise comparativa da síntese de hidroxiapatita via estado sólido. Matéria (Rio de Janeiro), v.25, p.1-13, 2020. https://doi.org/10.1590/S1517-707620200001.0914

Wang, Y.; Bi, G.; Cao, Z. Study on the wind speed of the different soil texture types in the Nenjiang Sandy Land. Protection Forest Science and Technology, v.4, p.1-2, 2007.

Wu, S. G.Soil Mechanics. Chongqing: Chongqing University Press, 2016. Cap.1, p.5-10.

Xiang, W.; Wu, M.; Lu, J.; Simulation physical parameter calibration of clay loam based on accumulation test. Transactions of the Chinese Society of Agricultural Engineering, v.35, p.116-123, 2019.

Xu, R.; Deng, Y.; Huang, Y.; Calculation theory of earth pressure considering particle contact area. Bulletin of Science and Technology, v.33, p.156-162, 2017.

Zeng, Z.; Ma, X.; Cao, X.; Application status and the prospect of discrete element method in agricultural engineering research. Transactions of the Chinese Society of Agricultural Machinery, v.52, p.1-20, 2021.

Zhou, J.; Su, J. A detailed explanation of ANSYS Workbench finite element analysis examples. Beijing: People's Posts and Telecommunications Press, 2017.255p.